

## Analysis of temperature, stress, and displacement distributions of staves for a blast furnace

Xiao-jun Ning, Shu-sen Cheng, and Ning-qiang Xie

School of Metallurgical and Ecological Engineering, University of Science and Technology Beijing, Beijing 100083, China  
(Received 2008-10-18)

**Abstract:** The temperature of gas flow inside a blast furnace (BF) changes significantly when the blast furnace is under unstable operations, and the temperature and stress distributions of cooling staves (CS) for BF work the same pattern. The effect of gas temperature on the temperature, stress, and displacement distributions of the cooling stave were analyzed as the gas temperature inside the blast furnace rose from 1000 to 1600°C in 900 s. The results show that both the temperature and temperature gradient of the hot side of CS increase when the gas flow temperature inside BF rises. The temperature gradient of the hot side of CS is greater than that of the other area of CS and it can reach 65°C/mm. In the vertical direction of the hot side of CS, closer to the central part of CS, the stress intensity is greater than that of the other area of the hot side of CS, which causes cracks on the hot side of CS in the vertical direction. As the gas temperature increases, the stress intensity rate near the fixed pin increases and finally reaches 45 MPa/s. Fatigues near the fixed pin and bolts are caused by great stress intensity rate and the area around the pin can be damaged easily. The edge of CS bends toward the cold side and the central part of CS shifts toward the hot surface.

**Key words:** blast furnace; cool stave; gas temperature; numerical simulation

[This work was financially supported by the National Natural Science Foundation of China (No.60672145).]

### 1. Introduction

The design and maintenance of cooling staves are pivotal factors related to the prolongation of campaign life of a blast furnace (BF). To further understand the working mechanism of cooling staves (CS), Cheng *et al.* carried out much research on CS ranging from thermal conductivity, installation of CS, to material properties and so on [1-7]. Shi *et al.* found out the reasons of destruction of CS from the heat transfer and stress aspects [8-10]. It is found that the gas flow inside BF changes significantly while the blast furnace is under unstable operations, and the temperature and stress fields of CS work the same pattern. It is necessary to figure out the temperature, stress, and displacement distributions of CS when the gas temperature changes.

In this paper, the temperature, stress, and displacement distributions of CS are analyzed, respectively, when the gas temperature inside a blast furnace increases 200°C every 300 s from 1000 to 1600°C, as

shown in Fig. 1.

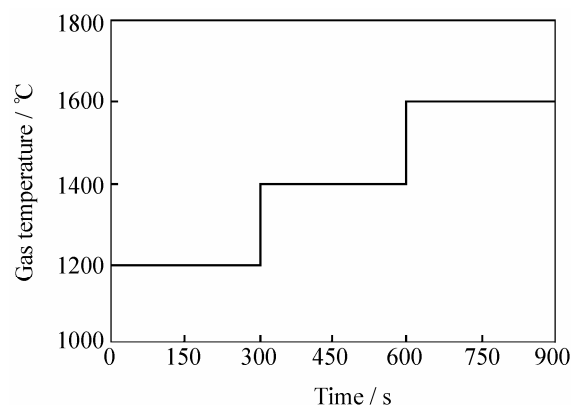


Fig. 1. Gas temperature curve.

### 2. Model descriptions

The three dimensional model of CS is shown in Fig. 2. The studied CS is located at the lower part of the furnace shaft of BF and the skull on the hot surface is so thin that it can be neglected. Considering the symmetrical features of CS, half of the actual stave is

studied to reduce the calculating speed. The structure is divided into the shell, packing, stove, and inlaid bricks, respectively, from the cold side to the hot side of CS, as shown in Fig. 2. There are four types of boundary conditions in the model: (1) the convective boundary that includes the interfaces between air and shell, cooling water and the inner surface of pipes, and hot surface and gas; (2) the adiabatic boundary that includes all surfaces on the model except convective boundaries; (3) the fixed pin completely fixed on the shell and bolts which are fixed on the shell but can move along the shell plane, as shown in Fig. 2; (4) free surfaces except those mentioned above. Considering the complex situation inside BF, the synthetic heat transfer coefficient (SCHTC) between gas and wall can be achieved from industrial experiments and calculation. The parameters of the model and thermal boundaries are listed in Tables 1 and 2. The rectangular coordinate of the model is shown in Fig. 2.

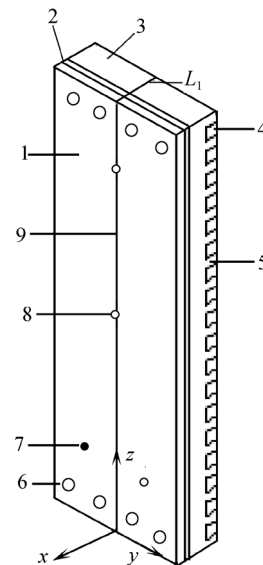


Fig. 2. Physical model: 1—shell; 2—packing; 3—stave; 4—inlaid brick; 5—rib; 6—water pipe; 7—fixed bolt; 8—fixed pin; 9—symmetrical surface.

Table 1. Model size

x axis	Shell	Packing	Packing to pipe	Pipe diameter	Pipe to rib	Rib
Thickness / m	0.050	0.030	0.030	0.065	0.035	0.070
y axis	Side face to pipe surface	Pipe diameter	Pipe centerline's interval	Pipe surface to side face		
Width / m	0.0725	0.065	0.210	0.0725		
z axis	Topside rib	brick	Rib	Downside rib		
Height / m	0.056	0.068	0.072	0.056		

Note: the model size is 2560 mm (height)×840 mm (width)×200 mm (thickness).

Table 2. Boundary conditions

Air temperature /°C	50
CHTC between air and shell / (W·m <sup>-2</sup> ·K <sup>-1</sup> )	12
Gas temperature /°C	1000, 1200, 1400, 1600
SCHTC between gas and wall / (W·m <sup>-2</sup> ·K <sup>-1</sup> )	232, 240, 250, 260
Cooling water temperature /°C	30
CHTC between cooling water and the internal surface of pipes / (W·m <sup>-2</sup> ·K <sup>-1</sup> )	8000

Note: CHTC—convective heat transfer coefficient.

### 3. Analysis of temperature field

#### 3.1. Temperature analysis in the thickness direction

The variation in temperature and temperature gradient on the topside from the hot side to the cold side of CS is shown in Fig. 3. The hot side temperature of CS is 477, 536, 632, and 740°C, respectively, when the time is 0, 300, 600, and 900 s. It is obvious that the temperature of CS increases as the gas temperature rises. From the hot side to the cold side, the temperature decreases gradually. On the cold side of CS, the temperature changes little with time. The temperature on the hot sides of CS increases greater because of its direct contact with gas. At 900 s, the temperature gradient reaches 65°C/mm approximately on the hot side of CS and this can cause great thermal stress in the

stave and make the stave in danger, which will be discussed later. If the gas temperature increases dramatically, CS could be destructed. Just as shown in Fig. 4, the downside part of CS is burnout due to the high temperature. It is important to make sure that the gas temperature is under the certain value, which means the operations of BF should be kept as stable as possible.

#### 3.2. Temperature analysis of different nodes

Fig. 5 shows that temperature changes with time at different two nodes on the hot side of CS. One node is located on the rib while the other on the inlaid brick. As shown in Fig. 5, temperatures at the two nodes increase when the gas temperature rises. Because of the different thermal conductivities between inlaid bricks and ribs, the difference in temperature between inlaid

bricks and ribs is high up to 110°C. When the gas temperature rises, the temperature rate (TR) of CS increases and the maximum value can reach 60°C/s, but when gas temperature is steady, the rate decreases to the minimum as 5°C/s. The TR of inlaid bricks is higher than that of ribs, so the effect of gas tempera-

ture is more obvious on inlaid bricks and may cause irrecoverable destruction of the bricks. As shown in Fig. 4, the inlaid bricks are burned-out completely. Keeping the gas temperature steady, which also means stable operation of BF, is important to decrease the damage of CS.

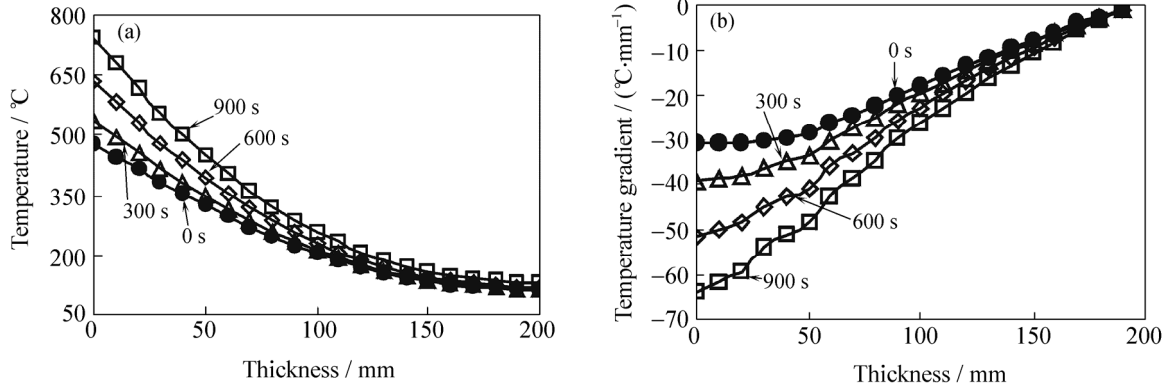


Fig. 3. Temperature and temperature gradient curves on the topside from the hot side to cold side of CS: (a) temperature curve; (b) temperature gradient curve.



Fig. 4. Damage of the stave for BF.

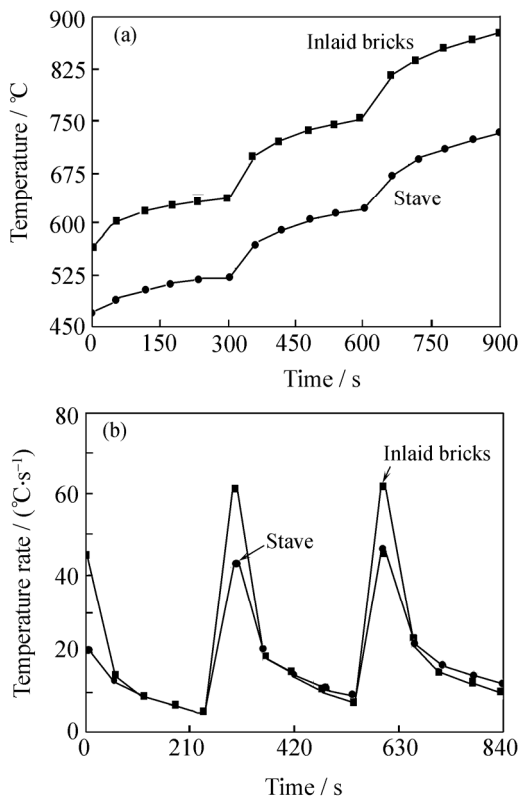


Fig. 5. Temperature and TR curves at the two nodes on the hot side: (a) temperature curves; (b) TR curves.

#### 4. Analysis of stress field

##### 4.1. Analysis of stress distribution

The distribution of stress intensity of CS is shown in Fig. 6 when gas temperature is 1000°C. The stress intensity on the cold side of CS, which is affected by the position of the water pipes and fixed pin, is less than that on the hot side. In the middle part of the vertical direction, the stress intensity is greater than that on the other area of the hot side of CS, as shown in Fig. 6. The stress intensity of inlaid bricks is less than that of ribs but more easily to be damaged than ribs due to their low yield stress, so the damage of inlaid bricks occurs earlier than that of ribs, as shown in Fig. 4. The maximum and minimum stress intensities are 400 and 10 MPa and located respectively on the hot sides of ribs and inlaid bricks.

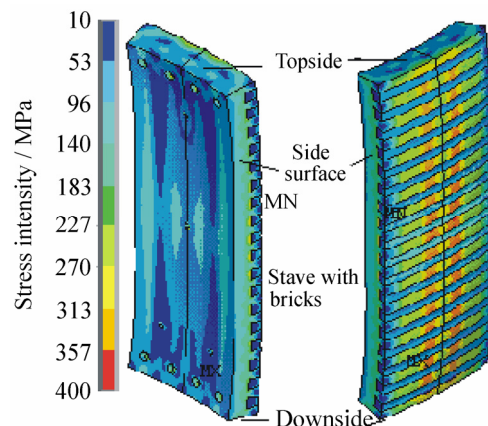


Fig. 6. Stress intensity contour.

The stress intensity distribution on the cross section of CS at a height of 1780 mm is shown in Fig. 7. The stress intensity between water pipes is less than that of

other regions.

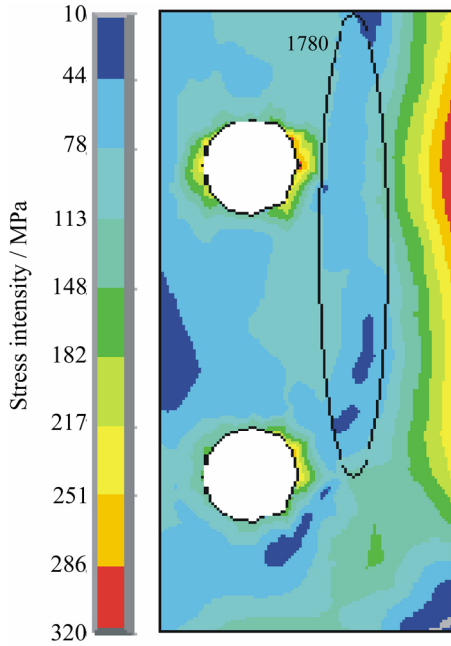


Fig. 7. Stress intensity contour on the cross section.

**4.2. Analysis of stress intensity at the thickness and width directions**

The stress intensity of ribs is greater than that of inlaid bricks and the former reaches 250 MPa, as shown in Fig. 8. On the cold side of CS, the stress in-

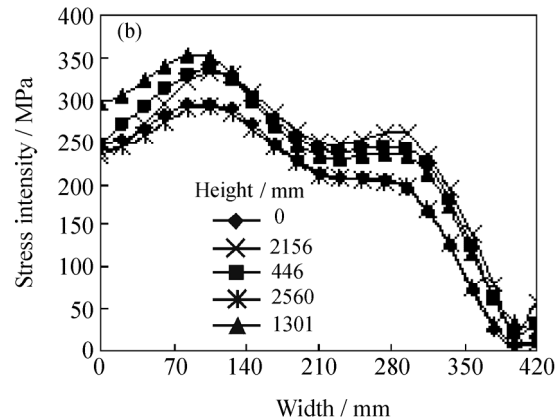
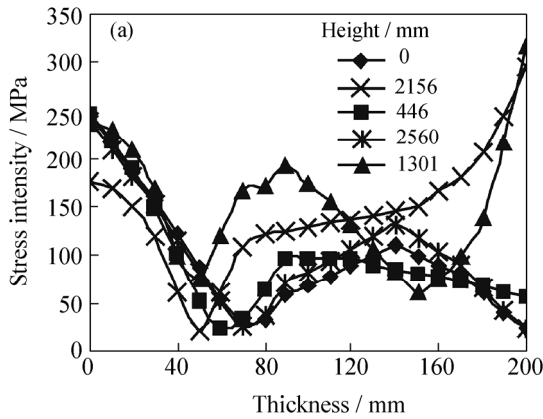


Fig. 8. Stress intensity distribution at different heights: (a) stress intensity curves in the thickness direction; (b) stress intensity curves in the width direction.

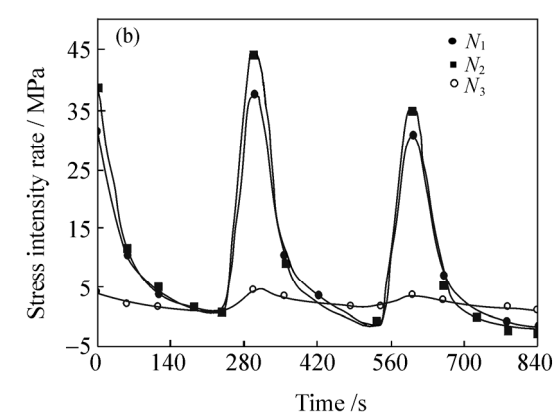
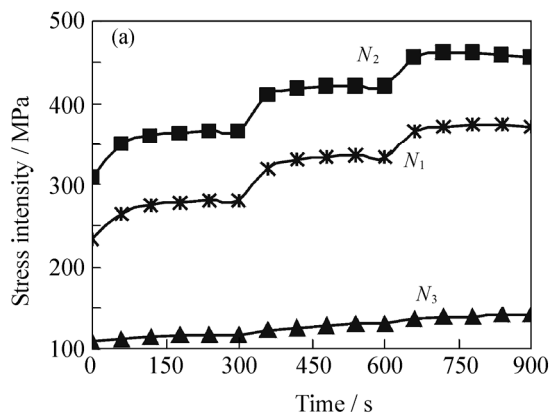


Fig. 9. Stress intensity curves on nodes: (a) stress intensity curves; (b) SIR curves.

tensity is much less (about 30 MPa). But the stress intensities around the fixed pin and bolts, whose heights are 1301 and 2156 mm, respectively, are both beyond 300 MPa and these regions are easily damaged considering the yield stress of the cast steel (about 350 MPa). As shown in Fig. 8(b), the stress intensity near the symmetrical line of the model is around 350 MPa and under 20 MPa on the side surface. So the regions near the symmetrical line are dangerous and should be paid more attention.

**4.3. Stress intensity on nodes**

Fig. 9(a) shows the changes in stress intensity at different three nodes whose coordinates are  $N_1(-280, 0, 2560)$ ,  $N_2(-280, 0, 1316)$ , and  $N_3(-280, 0, 1346)$ , respectively. The location of  $N_1$  and  $N_3$  is on the top-side and on the inlaid brick of the hot side of CS, while  $N_2$  locates near the fixed pin. As shown in the figure, stress intensity on the hot side of the rib ( $N_2$ ) is greater than that of the inlaid brick ( $N_3$ ) and topside ( $N_1$ ). As the gas temperature increases, the stress intensity rate (SIR) near the fixed pin increases and finally reaches 45 MPa/s, as shown in Fig. 9(b). This can cause the fatigue of ribs and shorten the life of CS. Considering the low yield stress of inlaid bricks, even the SIR of inlaid bricks ( $N_3$ ) is under 5 MPa/s, they can be damaged also.

#### 4.4. Displacement at nodes

The deformation of CS is similar (as shown in Fig. 6) when the gas temperature is changing. Fig. 10 shows the curves of displacement at different nodes that the coordinates are  $A(-280, 420, 2560)$  and  $B(-280, 420, 0)$ , respectively. The displacements at these two nodes become greater as the gas temperature

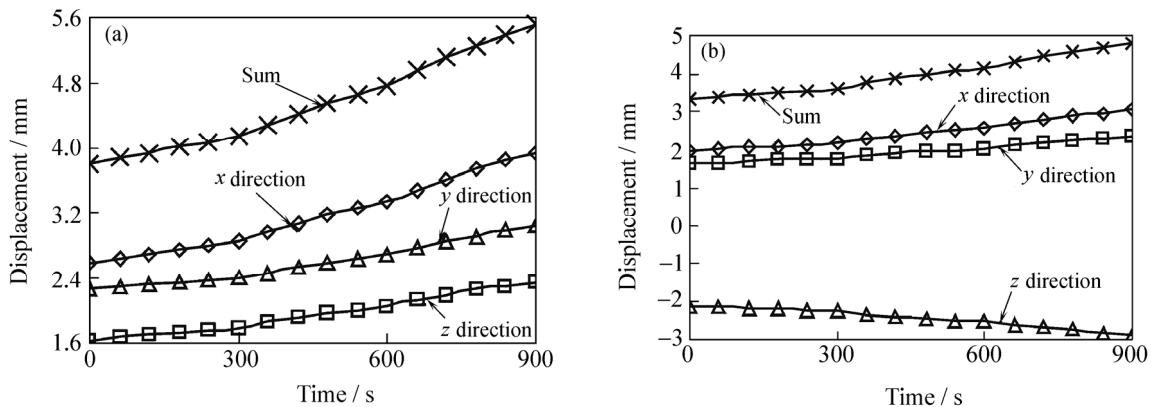


Fig. 10. Displacement curves at two nodes: (a) node A; (b) node B.

#### 5. Conclusions

(1) Both the temperature and temperature gradient of the hot side of CS increase when the temperature of gas flow inside BF rises. The temperature gradient of the hot side of CS is greater than that of other areas of CS and the temperature change of the cold side is too little to be taken into account. As the gas temperature rises, the temperature of CS increases and the rate near the hot side is above  $60^{\circ}\text{C}/\text{mm}$ . It is necessary to maintain stable operation of BF.

(2) Stress intensity on the cold side of CS is less due to the effect of water pipes and far from the hot side of CS. In the middle part of the vertical direction, the stress intensity is greater than that on the other area of the hot side of CS, which causes cracks on ribs in the vertical direction. Stress intensity around the fixed pin is so strong that these parts around the fixed pin can be damaged. As the gas temperature increases, the stress intensity rate near the fixed pin increases and finally reaches  $45\text{ MPa/s}$ . To avoid engendering much stress intensity, the fixed pin and bolts should be installed loosely and can move a little in the height and width directions.

(3) The edge of CS is bended to the cold sides and the middle part shifts to hot sides. The sum displacement in the  $z$  direction is  $6\text{ mm}$  and the interval between cooling staves should be above  $12\text{ mm}$  at least when they are installed.

#### References

[1] S.S. Cheng, Q.G. Xue, and D.Q. Cang, Heat transfer

increases. The packing between the staves and shell is used to release stress intensity and decrease the deformation of the shell and staves. The sum displacement in the  $z$  direction is  $6\text{ mm}$ . The interval between cooling staves should be above  $12\text{ mm}$  at least when they are installed.

- analysis of blast furnace stove, *Iron Steel* (in Chinese), 34(1999), No.5, p.11.
- [2] S.S. Cheng, T.J. Yang, and W.G. Yang, Analysis of heat transfer and temperature field of blast furnace copper stove, *Iron Steel* (in Chinese), 36(2001), No.2, p.8.
- [3] S.S. Cheng, *Comprehensive Technology on Long Campaign-ship of Blast Furnace* [Dissertation] (in Chinese), University of Science and Technology Beijing, Beijing, 1998.
- [4] S.S. Cheng, L. Sun, and T.J. Yang, Study on temperature field of cooling plate lining of blast furnace, *Iron Steel* (in Chinese), 39(2004), No.2, p.14.
- [5] S.S. Cheng, T.J. Yang, and Q.G. Xue, Analysis of computational heat transfer of the arrangement for the cooling apparatus on long campaign-ship blast furnace, *J. Univ. Sci. Technol. Beijing* (in Chinese), 24(2004), No.1, p.15.
- [6] L. Qian and S.S. Cheng, Realizing the self-protect ability of a blast furnace cooling system with copper stove, *J. Univ. Sci. Technol. Beijing* (in Chinese), 28(2006), No.11, p.1052.
- [7] X.J. Ning, S.S. Cheng, and N.Q. Xie, Thermal state experiment and analysis of thin copper cooling stove, *J. Univ. Sci. Technol. Beijing* (in Chinese), 29(2007), Suppl.2, p.126.
- [8] L. Shi, S.S. Cheng, and X.W. Ruan, Analysis of thermal performance of blast furnace cast copper stove, *Iron Steel* (in Chinese), 41(2006), No.6, p.13.
- [9] L. Shi and S.S. Cheng, Study of thermal distortion cast iron cooling stove with surface alloyed steel pipe, *Iron Steel* (in Chinese), 42(2007), No.11, p.9.
- [10] H.W. Pan, S.S. Cheng, and D.F. Wu, Study on thermal test and computational simulation of cast steel stove, *Ironmaking* (in Chinese), 26(2007), No.5, p.28.